

STUDY OF THE CHARACTERISTICS OF COUPLED HEAT TRANSFER NEAR SYMMETRY SURFACES OF BODIES WITH DIFFERENT SHAPE

V. I. Zinchenko and E. N. Putyatina

UDC 533.526+536.24

The results of a study of the characteristics of heat transfer accompanying flow around bodies of different shape at the angles of attack are presented.

There are a number of works devoted to the solution of the problems of coupled heat transfer with axisymmetric flow around bodies [1-3]; the effect of a nonisothermal temperature of the surface on the heat flux to the wall accompanying flow around flat bodies was studied in [4]. It is of interest to study nonstationary heat transfer accompanying supersonic flow of a perfect gas around differently shaped bodies at the angles of attack for different flow regimes in the boundary layer.

In accordance with [2, 3], we shall seek the characteristics of the coupled heat transfer from the solution of the equations describing the change in the averaged quantities in the boundary layer and the nonstationary heat conduction equation in the envelope of the body with the corresponding boundary and initial conditions.

We shall study a three-dimensional flow having a symmetry plane. We choose on the surface of the body in the flow a curvilinear nonorthogonal coordinate system centered on the stagnation point [5]. Then, from the general system of equations of a three-dimensional boundary layer [6], with the help of an expansion accurate up to second-order infinitesimals in the circumferential coordinate it is possible to write out the system of equations for the boundary layer near the symmetry plane; after the introduction of the stream functions f and φ and the Dorodnitsyn-Liz variables, using the notation adopted in [5], it assumes the form

$$\frac{\partial}{\partial \zeta} \left(l_{\Sigma} \frac{\partial^2 f}{\partial \zeta^2} \right) + (f + \alpha_2 \varphi) \frac{\partial^2 f}{\partial \zeta^2} = \alpha_1 \left(\frac{\partial f}{\partial \zeta} \frac{\partial^2 f}{\partial s \partial \zeta} - \frac{\partial f}{\partial s} \frac{\partial^2 f}{\partial \zeta^2} \right) + \beta_1 \left[\left(\frac{\partial f}{\partial \zeta} \right)^2 - \frac{\rho_e}{\rho} \right], \quad (1)$$

$$\begin{aligned} \frac{\partial}{\partial \zeta} \left(l_{\Sigma} \frac{\partial^2 \varphi}{\partial \zeta^2} \right) + (f + \alpha_2 \varphi) \frac{\partial^2 \varphi}{\partial \zeta^2} = \alpha_1 \left(\frac{\partial f}{\partial \zeta} \frac{\partial^2 \varphi}{\partial s \partial \zeta} - \frac{\partial f}{\partial s} \frac{\partial^2 \varphi}{\partial \zeta^2} \right) + \\ + \beta_2 \left[\left(\frac{\partial \varphi}{\partial \zeta} \right)^2 - \frac{\rho_e}{\rho} \right] + \beta_3 \left[\left(\frac{\partial f}{\partial \zeta} \right)^2 - \frac{\rho_e}{\rho} \right] + \beta_4 \left[\frac{\partial f}{\partial \zeta} \frac{\partial \varphi}{\partial \zeta} - \frac{\rho_e}{\rho} \right], \end{aligned} \quad (2)$$

$$\frac{\partial}{\partial \zeta} \left\{ \frac{l_{\Sigma}}{\text{Pr}_{\Sigma}} \frac{\partial g}{\partial \zeta} + \frac{(u_e^0)^2}{2H_e} l_{\Sigma} \left(1 - \frac{1}{\text{Pr}_{\Sigma}} \right) \frac{\partial}{\partial \zeta} \left[\left(\frac{\partial f}{\partial \zeta} \right)^2 \right] \right\} + (f + \alpha_2 \varphi) \frac{\partial g}{\partial \zeta} = \alpha_1 \left(\frac{\partial f}{\partial \zeta} \frac{\partial g}{\partial s} - \frac{\partial f}{\partial s} \frac{\partial g}{\partial \zeta} \right). \quad (3)$$

Assuming the process is one-dimensional, the nonstationary equation of heat conduction in the material of the body in an orthogonal coordinate system tied to the symmetry axis of a body of revolution has the form

$$\pi_p \frac{\partial \Theta}{\partial \tau} = \frac{1}{H_1 r_1} \frac{\partial}{\partial n_1} \left[H_1 r_1 \pi_1 \frac{\partial \Theta}{\partial n_1} \right]. \quad (4)$$

The boundary and initial conditions are written as follows:

$$\frac{\partial f}{\partial \zeta} (\infty, s) = 1, \quad \frac{\partial \varphi}{\partial \zeta} (\infty, s) = 1, \quad g(\infty, s) = 1, \quad (5)$$

$$\frac{\partial f}{\partial \zeta} (0, s) = \frac{\partial \varphi}{\partial \zeta} (0, s) = 0, \quad f(0, s) = \varphi(0, s) = 0, \quad (6)$$

$$q_w(0, s) \sqrt{\text{Re}} \text{Pr} \frac{\lambda_{e0}}{\lambda_{1*}} - \pi_0 \Theta_w^4 = \pi_1(\Theta_w) \frac{\partial \Theta_1}{\partial n_1}(\tau, 0),$$

$$\frac{\partial \Theta}{\partial n_1} \left(\tau, \frac{L}{R_N} \right) = 0 \quad \text{or} \quad \Theta \left(\tau, \frac{L}{R_N} \right) = \Theta_H, \quad (7)$$

$$\Theta(0, n_1) = \Theta_H. \quad (8)$$

The three-dimensional turbulent flow is described with the help of a two-layer model of a turbulent boundary layer [7], presented in [5].

In the transitional region from the laminar regime to the turbulent regime the flow was calculated as in [5] using the coefficient of longitudinal intermittency [8, 9].

The pressure distribution on the outer boundary of the boundary layer was fixed by Newton's formula: $p_e/p_{e0} = \cos^2 \theta = \left(\frac{v_{n\infty}}{v_\infty} \right)^2$, where θ is the angle between the velocity vector of the incoming flow and the normal to the surface at a running point.

The relations for calculating the quantities on the outer boundary of the boundary layer as well as the coefficients of the asymptotic system of equations in the vicinity of the stagnation point are given in [5].

The boundary-value problem (1)-(8) was integrated numerically with the help of the iteration-interpolation method of [10]. The general method for calculating the coupled problem follows from the quasistationary formulation in the gas phase and is linked with the systematic solution of the system of equations in the gas phase and the equations of heat conduction in the body [2].

In carrying out the numerical calculations the shape of the bodies in the flow (second-order surfaces were studied), the angles of attack, the Re number, and the coupling parameter $S = \sqrt{\text{Re}} \text{Pr} \frac{\lambda_{e0}}{\lambda_{1*}}$ were varied. The thermophysical characteristics of the material were assumed to be constants; $\text{Pr} = 0.72$ and $\text{Pr}_T = 1$.

We shall examine the results of the solution of the boundary value problem (1)-(8) for the case of laminar flow in the boundary layer. Figure 1a shows the distributions of the dimensionless heat flux q_w and the surface temperature $\Theta_w(\xi) = T_w/T_{e0}$ along the plane of symmetry of an ellipsoid of revolution, oriented in the flow at an angle of attack $\alpha = 10^\circ$, at different times. Here ξ is the length of the arc measured from the symmetry axis of the body while the x 's denote the values at the stagnation points. The equation of the surface in the flow in a Cartesian coordinate system tied to the symmetry plane has the form $k^2 x_s^2 + y_s^2 + z_s^2 = 1$, where k is the ratio of the semiaxes.

The solid curves in Fig. 1 were obtained for an ellipsoid with $k = 3.07$; the broken curves were obtained for an ellipsoid with $k = 0.5$. Here $\mu/\mu_e = \sqrt{T/T_e}$, $T_{e0} = 1210$ K, $\Theta_H = 0.248$, $S = 3.186$, $L/R_N = 0.1$, $\frac{\partial \Theta_1}{\partial n_1} |_{n_1=L/R_N} = 0$. For oblate ellipsoids ($k > 1$), oriented in the flow under different angles of attack ($0 \leq \alpha \leq 30^\circ$), the maximum of the initial value of q_w is realized on the lateral surface on the upstream side of the flow, which with time leads to a maximum surface temperature in this region. For prolate ellipsoids (broken curves) oriented at moderate angles of attack the maximum heat flux and therefore the maximum surface temperature are realized at the stagnation point; increasing the angle of attack to $20-30^\circ$ leads to some shift in the maxima of q_w and Θ_w from the point of stagnation on the downstream side toward the point of the maximum curvature of the generatrix of the body in the flow $x_s = 1/k$, $y_s = z_s = 0$.

Near the plane of symmetry the following formula was obtained for the ratio of the heat fluxes with the help of the method of successive approximations [11, 12] for the case of a non-isothermal surface:

$$\frac{q_w(s)}{q_w(0)} = \sqrt{\frac{\rho_e^0 \mu_e^0 \mu_e^0}{2 \frac{du_e^0}{ds} \Big|_{s=0} \alpha_1 \rho_{e0} \mu_{e0}}} \left\{ \frac{(1-\gamma) B_\infty(0)}{B_\infty(s)} \sqrt{\frac{\delta_g(0)}{\delta_g(s)}} + \right.$$

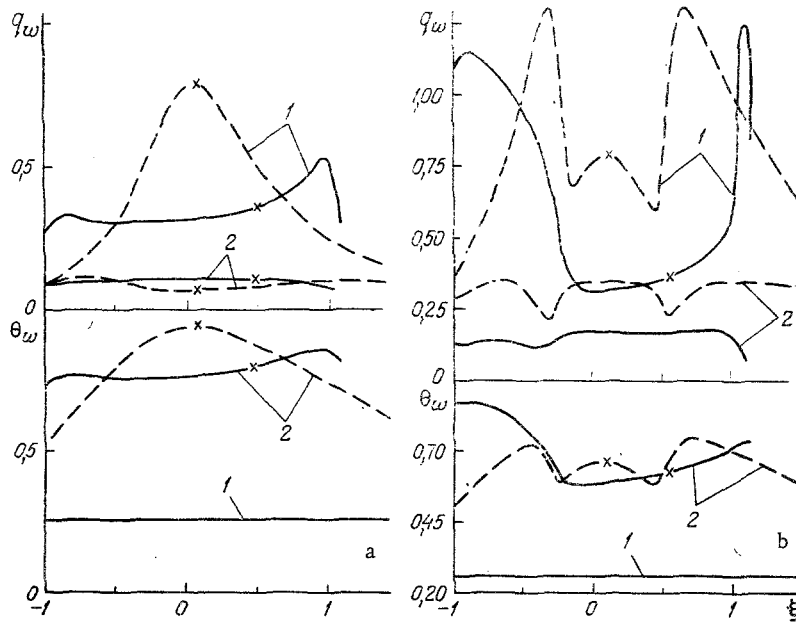


Fig. 1. Distribution of the dimensionless heat flux and surface temperature along the plane of symmetry at different times: a) $\tau = 0$ (1) and 0.02 (2); b) $\tau = 0$ (1) and 0.01 (2).

$$\begin{aligned}
 & + 2\text{Pr} \sqrt{\delta_g(s) \delta_g(0)} B_\infty(0) \alpha_1 \beta \left[1 - \frac{\Phi_1}{2B_\infty(s)} \right] \frac{1 - \Theta_w(s)}{1 - \Theta_w(0)}, \\
 & \beta = \frac{\partial \ln(1 - \Theta_w)}{\partial s}, \quad \Phi_1 = 0,068 + 0,091A, \quad A = \left[\frac{\Theta_w}{1 - \frac{(u_e^0)^2}{2H_{e0}}} \right]^{1/2}, \\
 & \chi = \rho_e^0 \mu_e^0 u_e^0 \left(\frac{r_w}{R_N} \right)^2, \quad \gamma = \frac{(1 - \text{Pr})}{(1 - \Theta_w)} \frac{(u_e^0)^2}{2H_{e0}}, \quad B_\infty = 0,068 + 0,057A, \\
 & E = \exp \left(2 \int_0^s \frac{\omega_e^0 R_N}{u_e^0 r_w^0} ds \right), \\
 & \delta_g(s) = \left[\int_0^s \frac{(1 - \gamma) \chi E}{\text{Pr} B_\infty(s)} \exp \left(\int_0^s \beta \frac{\Phi_1}{B_\infty} ds \right) ds \right] \left[\alpha_1 \chi E \exp \left(\int_0^s \beta \frac{\Phi_1}{B_\infty} ds \right) \right]^{-1}.
 \end{aligned} \tag{9}$$

Here $q_w(0)$ corresponds to the heat flux at the point of stagnation; $\delta_g(0)$, can be written as follows using the expansion of the functions near the critical point:

$$\delta_g(0) = \frac{1}{\text{Pr} B_\infty(0) \left(1 + \frac{R_1(0)}{R_2(0)} \right)}, \quad B_\infty(0) = 0,068 + 0,057\Theta_w^{1/2}. \tag{10}$$

It follows from an analysis of the formula (9) as well as the results of the numerical calculations that the second term associated with the derivative $\partial \Theta_w / \partial s$, can make a significant contribution to the value of the coefficient of heat transfer in the case of a nonisothermal surface, while the parametric excess of the values $\Theta_w = \text{const}$ has virtually no effect on the ratio $q_w(s)/q_w(0)$. The effect of the nonisothermal nature of the surface temperature on the heat-transfer coefficient is shown in Fig. 2a, which shows an analysis of the numerical

solution, given in Fig. 1a, in the form of the ratio of the numbers $St/St(0) = \frac{q_w(s)}{1 - \Theta_w(s)} / \frac{q_w(0)}{1 - \Theta_w(0)}$ for different times. Here, like in Fig. 1a, the broken curves correspond to $k = 0.5$,

the solid curves correspond to $k = 3.07$, the curves 1 were obtained for $\tau = 0$, $\theta_w = \theta_n = \text{const}$, the curves correspond to $\tau = 0.02$ and variable surface temperature, and the dots are the data obtained for $\tau = 0$ from the formula (9). As follows from Fig. 2a, for constant and variable surface temperatures the values of $St/St(0)$ can differ significantly. In regions of positive gradients $\partial\theta_w/\partial s$ the numbers St/St_0 decrease, while for negative values of $\partial\theta_w/\partial s$ they increase compared with the isothermal case in accordance with (9). This can lead to a significant underestimation of the surface temperature in the regions where $\partial\theta_w/\partial s < 0$ in the calculation of the temperature field in the body using the coefficient of heat transfer from the gas phase for the case $\theta_w = \text{const}$. Analogous results are presented in [4], where subsonic flow around nonisothermal bodies was studied.

Comparison of the results of the solution of the exactly formulated problem taking into account the coupled heat transfer (curves 1) with the results of the solution of a separately formulated problem are presented in Figs. 2b and c for $\tau = 0.02$. Here and in Fig. 3 the curves 2 correspond to the solution of the heat conduction equation with a fixed heat flux from the

gas phase in the form $q_w(s) = \frac{q_w(s)}{q_w(0)} q_w(0)$, where the ratio $q_w(s)/q_w(0)$ was taken from (9),

while the heat flux $q_w(0)$ was calculated using the formula [12]:

$$q_w(0) = \frac{q_w(0)}{q_w^0(0)} q_w^0(0). \quad (11)$$

Here $q_w(0)/q_w^0(0) = \sqrt{\frac{1}{2} \left(1 + \frac{R_1(0)}{R_2(0)}\right)}$, $q_w^0(0)$ is the value of the heat flux near the critical

point with axisymmetric flow, for which the well-known formulas of [13], written out for the case of a perfect gas, were employed. The curves 3 correspond to the case when the second term in the formula (9) was neglected, i.e., $\beta = 0$; the expression for $\delta_g(s)$ was also simplified.

The curves 4 were obtained for the case when the expression $q_w(s) = \left(\frac{q_w(s)}{q_w(0)}\right)^0 q_w(0)$, where

$\left(\frac{q_w(s)}{q_w(0)}\right)^0$ was chosen for the starting isothermal temperature of the surface, was employed for

the heat flux from the gas phase. The curves 5 were obtained using the flux $q_w(s) = \frac{St(s)}{St(0)}$

$\frac{[1 - \theta_w(s)]}{[1 - \theta_w(0)]} q_w(0)$ where the ratio $St(s)/St(0)$ was taken in front of θ_{wH} . We note that the

curves 4 and 5 correspond to fixing the coefficient of heat transfer from the gas phase for an isothermal surface.

As follows from a comparison of the curves $\theta_w(s)$, the results of the solution of the problem in the exact and uncoupled formulations are in fairly good agreement, if the formulas (9) are employed for the heat flux. If in fixing the heat flux from the gas phase only the history of the development of the thermal boundary layer is taken into account and the value of the local derivative $\partial\theta_w/\partial s$ is neglected, then the surface temperature is underestimated for those regions where $\partial\theta_w/\partial s < 0$. In addition, for oblate ellipsoids the maximum discrepancy in θ_w is observed on the upstream side and reaches, for example, 15% for $k = 3.07$ in the section $\xi = 1.07$, while for prolate ellipsoids this maximum discrepancy with respect to the surface temperature is realized on the downstream side and equals 13% for $k = 0.5$ in the section $\xi = -0.97$. In this case, if in the uncoupled formulation of the problem the coefficient of heat transfer from the gas phase is fixed for an isothermal surface, the error is substantially higher in this approach (curves 4).

Figure 3 shows the dynamics of the variation of the surface temperature as a function of time for the exact and separate formulations of the problems. As follows from the figure, the differences in the determination of the surface temperature based on the approaches studied increased with time.

It should be noted that starting with some value of s , corresponding to a change in the direction of flow relative to the symmetry plane, the error of the formulas (9) increases substantially and therefore the error in the determination of θ_w with the help of the approximate approaches based on the uncoupled formulation also increases significantly.

The calculation of the boundary-value problem (1)-(8) showed that for the adiabatic condition on the inner wall of the envelope for large values of τ the temperature across the en-

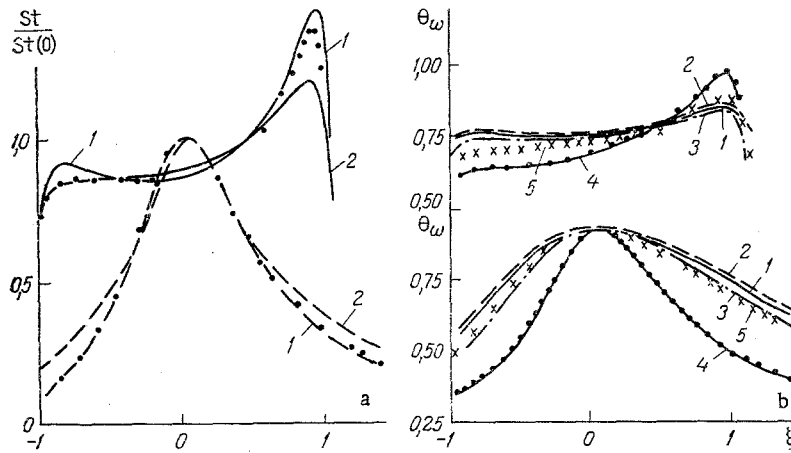


Fig. 2. Relative Stanton number and the surface temperature along the plane of symmetry at different times: a) $\tau = 0$ (1) and 0.02 (2); b) $k = 3.07$; c) $k = 0.5$.

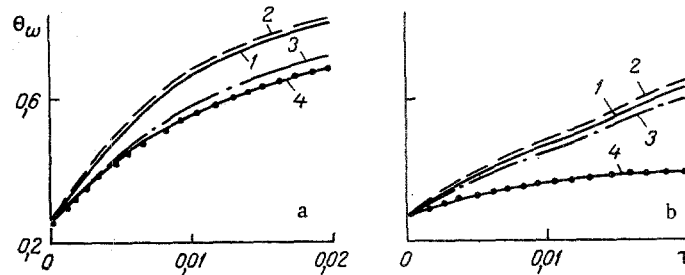


Fig. 3. Surface temperature as a function of time for different values of ξ : a) $k = 3.07$ and b) 0.5 .

velope is equalized and equals the radiative equilibrium temperature, which was determined independently from the problem (1)-(3), (5), and (6) with the balance equation for conservation of energy:

$$q_w(0, s) \sqrt{\text{Re}} \text{Pr} \frac{\lambda_{e0}}{\lambda_{1*}} = \pi_{\sigma} \theta_{wr}^4. \quad (12)$$

For $\varepsilon = 0.7$ and the computed data in Fig. 1a the parameter π_{σ} is small, and the distribution θ_{wr} is close to the value of the adiabatic surface temperature θ_{wa} . As the stagnation temperature T_{e0} increases π_{σ} increases and θ_{wr} decreases compared with θ_{wa} and varies along the circumference much more strongly.

Figure 4a shows, according to the results of Fig. 1a for $k = 3.07$, the dependence of the ratio of the Stanton numbers

$$\text{St}/\text{St}_i = \frac{q_w(s) [1 - \theta_{wi}(s)]}{[1 - \theta_w(s)] q_{wi}(s)}$$

on θ_w , where St_i corresponds to the starting isothermal surface temperature, for different values of the coordinate along the circumference of the body. The broken curves of St/St_i correspond to the results of the integration of the system of boundary-layer equations for different isothermal values of θ_w .

In the vicinity of the point of stagnation (curves 1) the computational results based on both formulations are in agreement; on the lateral surface they can differ qualitatively. For this reason, as pointed out above, the use of the law of heat transfer for an isothermal wall will lead to significant errors in θ_w on the upstream and downstream sides.

We shall examine the results of the solution of the boundary value problem in the presence of laminar, transitional, and turbulent regions of flow in the boundary layer. Figure 1b shows the behavior of $q_w(\xi)$, $\theta_w(\xi)$ for $\text{Re} = 5.7 \cdot 10^6$. Comparison of Figs. 1a and b shows

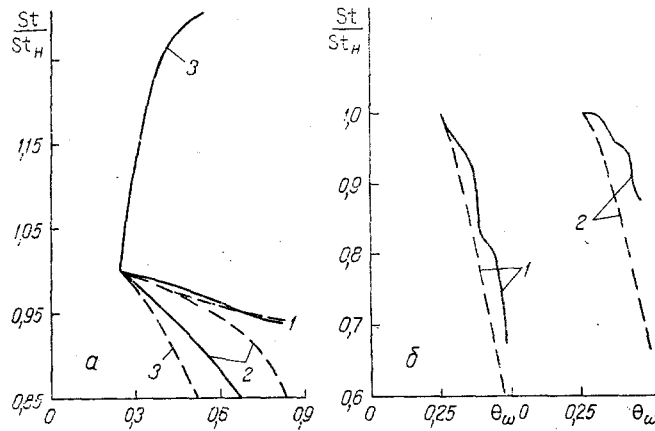


Fig. 4. Relative Stanton number St/St_H versus the surface temperature in different sections ξ ($k = 3.07$); a) $\xi = 0.47$ (1), 0.97 (2), 1.07 (3); b) $\xi = 1.037$ (1), 1.075 (2).

that in the region of a developed turbulent flow the heat fluxes are significantly stronger than the corresponding initial values for the laminar boundary layer. It is important to note that in this case the maximum heat fluxes to the body, reached on the upstream side, are close for different shapes of the blunt end, unlike the laminar flow regime. As the calculation showed, for oblate spheroids with $k \geq 2$ the region where the maximum heat fluxes are reached shifts insignificantly compared with the zone of the maximum of $q_w(s)$ for the laminar flow regime, while changing the angles of attack up to 15° has virtually no effect on the value and position of the maximum heat flux. We note that for large Re numbers, like in the case of axisymmetric flow, the position and magnitude of the maximum heat flux is independent of whether or not the transitional flow region is taken into account.

The above-noted features of the behavior of the heat flux along the generatrix for an isothermal surface determine in the solution of the coupled problem the distribution of the surface temperature of the body. As follows from Fig. 1b, the values of the maximum temperatures of the surface for the up- and downstream sides with $k = 0.5$ at different times are close, while the qualitative change in the behavior of $\theta_w(s, \tau)$ compared with Fig. 1a is a result of the change in the flow regimes.

For an oblate ellipsoid ($k = 3.07$) the temperature on the downstream side exceeds with time the level θ_w on the upstream side. This is attributable to the fact that as the temperature factor θ_w increases (both in the solution of the problem with heating and in the case $T = \text{const}$) laminar and transitional flow regions, for which the coefficient of longitudinal intermittency Γ is much less than 1, are observed on the studied part of the upstream side. On the downstream side the coefficient of intermittency Γ increases from 0 to 1 as the point of instability moves along the symmetry plane and reaches the developed turbulent flow regime with larger values of q_w than on the upstream side.

It is obvious that to find $q_w(s)$ it is important to have a criterion for determining the point of instability and the coefficient of intermittency Γ , and for this reason it is important to have additional information in order to refine their values for the case of three-dimensional flow in the boundary layer.

The results of the calculation performed for $k = 3.07$ are presented in Fig. 4 in the form of the dependence $St/St_H(\theta_w)$. The broken curves show the data from the numerical integration of the system of equations of a turbulent boundary layer for isothermal values for the wall. One can see that in this case the qualitative similarity in the behavior of the curves is preserved, but the quantitative difference is significant. For this reason the use of the law of heat transfer, found for the case of an isothermal wall, can also lead to a significant underestimation of the surface temperature. Analysis of the magnitude of the heat flux, performed in [4], showed that $q_w(s)$ for the turbulent flow regime also depends on $\partial T_w / \partial s$, but this dependence is weaker than in the case of a laminar boundary layer.

NOTATION

f and φ , dimensionless stream functions; $\partial f / \partial \zeta = u/u_e$, $\partial \varphi / \partial \zeta = \omega/\omega_e$, dimensionless velocity components; $g = H/H_{e0}$, dimensionless enthalpy; $\pi_1 = \lambda_1/\lambda_{1*}$, $\pi_\rho = \rho_1 c_1 / \rho_{1*} c_{1*}$, $\pi_\sigma =$

$\varepsilon \sigma T_{e0}^3 / \lambda_{1*}$, dimensionless parameters; $Re = \rho_{e0} v_m R_N / \mu_{e0}$, $v_m = \sqrt{2H_{e0}}$, $q_w = \lambda_w \left. \frac{\partial T}{\partial y} \right|_w \frac{\sqrt{Re}}{v_m \rho_{e0} H_{e0}}$ Reynolds

number, the maximum velocity, and the dimensionless heat flux; $\tau = t/t_*$, $\theta = T/T_{e0}$, dimensionless time and temperature; $t_* = R_N \rho_{1*} c_{1*} / \lambda_{1*}$, characteristic time; R_N and L , characteristic size and thickness of the envelope; $H_1 = 1 - h_1/R$, $r_1 = r_{w1} - n_1 \cos \alpha$, Lamé coefficients, where r_{w1} is the distance from the axis of symmetry to the generatrix; R , radius of curvature of the generatrix; α , angle formed by the generatrix and the symmetry axis; $n_1 = -n/R_N$, where n is the normal to the outer contour of the envelope. The indices e , $e0$, and w correspond to quantities on the outer boundary of the boundary layer, on the outer boundary at the point of stagnation, and on the surface of the body. The index 1 corresponds to the characteristics of the solid body and $*$ denotes characteristic values.

LITERATURE CITED

1. A. V. Lykov, Handbook of Heat and Mass Transfer [in Russian], Moscow (1972).
2. V. I. Zinchenko and E. G. Trofimchuk, Izv. Akad. Nauk SSSR, Mekh. Zhidk. Gaza., No. 4, 59-64 (1977).
3. V. I. Zinchenko and E. N. Putyatina, Inzh.-Fiz. Zh., 45, No. 1, 11-21 (1983).
4. A. Sh. Dorfman, Heat Transfer Accompanying Flow Around Nonisothermal Bodies [in Russian], Moscow (1982).
5. V. I. Zinchenko and E. N. Putyatina, Inzh.-Fiz. Zh., 50, No. 1, 5-14 (1986).
6. V. A. Aleksin and Yu. D. Shevelev, Izv. Akad. Nauk SSR, Mekh. Zhidk. Gaza., 2, 39-47 (1983).
7. T. Cebeci, AIAA J., 12, No. 6, 779-786 (1974).
8. K. K. Chen and N. A. Thyson, AIAA J., 9, No. 5, 63-68 (1971).
9. N. P. Kolina and E. E. Solodkin, Tr. TsAGI, No. 2046, 66-154 (1980).
10. A. M. Grishin and V. N. Bertsun, Dokl. Akad. Nauk SSR, 214, No. 4, 751-754 (1974).
11. G. A. Tirskii, "Method of successive approximations for integration of the equations of a laminar multicomponent boundary layer with chemical reactions, including ionization reactions," Report No. 1016, Institute of Mechanics, Moscow State Univ., (1969).
12. I. G. Brykina, É. A. Gershbein, and S. V. Peigin, Izv. Akad. Nauk SSSR, Mekh. Zhidk. Gaza, No. 5, 37-48 (1980).
13. D. Fay and F. Riddell, Gas-Dynamics and Heat Transfer in the Presence of Chemical Reactions [Russian translation], Moscow (1962), pp. 190-228.